

# UC Berkeley

## UC Berkeley Previously Published Works

### Title

Ring-Cleavage Products Produced during the Initial Phase of Oxidative Treatment of Alkyl-Substituted Aromatic Compounds

### Permalink

<https://escholarship.org/uc/item/2m99w32d>

### Journal

Environmental Science and Technology, 54(13)

### ISSN

0013-936X

### Authors

Van Buren, Jean  
Prasse, Carsten  
Marron, Emily L  
[et al.](#)

### Publication Date

2020-07-07

### DOI

10.1021/acs.est.0c00432

Peer reviewed



# HHS Public Access

Author manuscript

*Environ Sci Technol.* Author manuscript; available in PMC 2021 July 07.

Published in final edited form as:

*Environ Sci Technol.* 2020 July 07; 54(13): 8352–8361. doi:10.1021/acs.est.0c00432.

## Ring-Cleavage Products Produced During the Initial Phase of Oxidative Treatment of Alkyl-Substituted Aromatic Compounds

Jean Van Buren<sup>†</sup>, Carsten Prasse<sup>§</sup>, Emily L. Marron<sup>‡</sup>, Brighton Skeel<sup>†</sup>, David L. Sedlak<sup>†,‡</sup>

<sup>†</sup>Department of Chemistry, University of California at Berkeley, Berkeley, CA 94720, USA

<sup>§</sup>Department of Environmental Health and Engineering, Johns Hopkins University, Baltimore, MD 21218, USA

<sup>‡</sup>Department of Civil and Environmental Engineering, University of California at Berkeley, Berkeley, CA 94720, USA

### Abstract

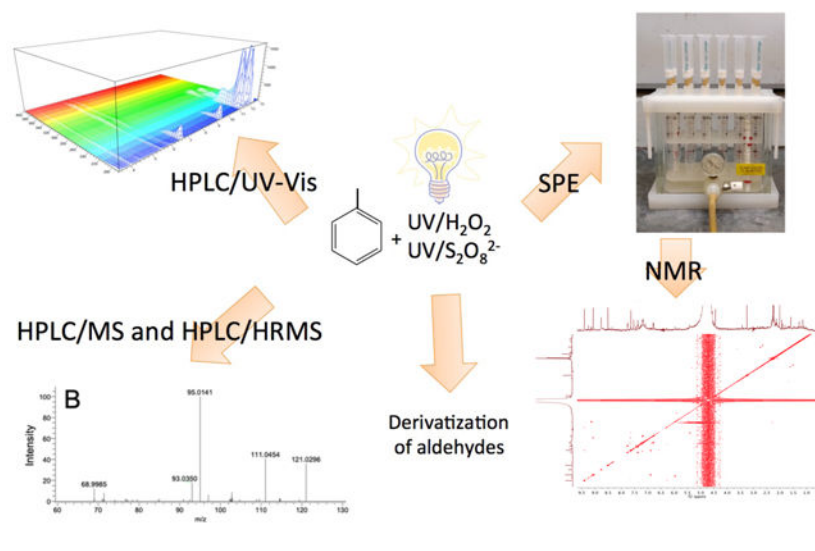
Chemical oxidation with hydroxyl radical (HO<sup>•</sup>) and sulfate radical (SO<sub>4</sub><sup>•-</sup>) is often used to treat water contaminated with aromatic compounds. Although oxidation of aromatics by these radicals has been studied for decades, the commonly accepted transformation pathway – sequential hydroxylation of the ring followed by ring cleavage and mineralization of the resulting products – does not account for the loss of the parent compound observed during the initial phase of the process. To assess the importance of pathways for aromatic compound oxidation that do not result in ring hydroxylation, we identified products formed after the initial reaction between HO<sup>•</sup> or SO<sub>4</sub><sup>•-</sup> and benzene, toluene, ethylbenzene, and xylene isomers. We quantified products of ring hydroxylation and oxidation of alkyl substituents as well as a suite of ring cleavage products, including acetaldehyde, formic acid, 6-, 7- or 8-carbon oxoaldehydes and oxodials. Other ring cleavage products, which were most likely aldehydes and organic acids, were observed but not quantified. When SO<sub>4</sub><sup>•-</sup> was used as the oxidant, aromatic organosulfates also were formed. Our results indicated that the initial phase of the oxidation process involves radical addition, hydrogen abstraction, or one-electron transfer to the ring followed by reaction with O<sub>2</sub>. The hydroxycyclohexadienylperoxy radical produced in this reaction can eliminate hydroperoxyl radical (HO<sub>2</sub><sup>•</sup>) to produce a phenolic compound or it can rearrange to form a bicyclic peroxy intermediate that subsequently undergoes ring cleavage. Hydroxylation of the ring and oxidation of the alkyl substituent accounted for approximately 15 to 40% of the reacted mass of parent compound. Ring cleavage products for which quantification was possible accounted for approximately 2 to 10% of the reacted mass. Our results raise concerns about the formation of toxic ring cleavage products during the initial stage of oxidation whenever HO<sup>•</sup> or SO<sub>4</sub><sup>•-</sup> are used for treatment of water containing benzene or alkylbenzenes.

### Graphical Abstract

<sup>†</sup>Corresponding author, phone 510-643-0256; fax 510-642-5319; sedlak@berkeley.edu.

The Supporting Information is available free of charge on the ACS Publications website at DOI: [10.1021/acs.est.0c00432](https://doi.org/10.1021/acs.est.0c00432).

Details of analytical methods for analysis of aldehydes, carbonyl compounds and aromatic compounds, detailed data on product yields, NMR spectra of transformation products, LC-HRMS spectra and HPLC/UV/Vis chromatograms of transformation products.



## Introduction

Hydrogen peroxide ( $\text{H}_2\text{O}_2$ ) and peroxydisulfate ( $\text{S}_2\text{O}_8^{2-}$ ) contain peroxide bonds that can be activated by reaction with catalysts, transition metals, ultraviolet light, or heat to produce hydroxyl radical ( $\text{HO}^\bullet$ ) and sulfate radical ( $\text{SO}_4^{\bullet-}$ ), respectively.<sup>1-4</sup> Due to their high reactivity with organic contaminants, these oxidants have found applications in the treatment of groundwater, surface water, and recycled water.<sup>2</sup> For example, over 200 sites with contaminated groundwater have been remediated by in situ chemical oxidation (ISCO) with  $\text{H}_2\text{O}_2$  or  $\text{S}_2\text{O}_8^{2-}$ ,<sup>5</sup> with the peroxide bonds undergoing activation by reaction with transition metals and metal oxides on aquifer solids, or in the case of  $\text{S}_2\text{O}_8^{2-}$ , thermal activation.<sup>6-8</sup> Photolytic cleavage of the peroxide bond in  $\text{H}_2\text{O}_2$  followed by oxidation with  $\text{HO}^\bullet$  is one of the main approaches for removing chemical contaminants in potable water reuse systems.<sup>9</sup>

Due to their widespread occurrence, high toxicity, and resistance to biotransformation, benzene and its methyl- and ethyl-substituted derivatives (i.e., BTEX compounds) are among the most common contaminants of concern for potential drinking water sources.<sup>10</sup> Hydroxyl radical attack on aromatic compounds, which has been studied since the 1960s,<sup>11,12</sup> involves electron transfer, H-abstraction, and addition to the aromatic ring. For most aromatic compounds, the primary reaction mechanism is believed to involve addition of  $\text{HO}^\bullet$  to the ring, in a reaction that proceeds at near diffusion-controlled rates.<sup>11,13</sup> The addition of  $\text{HO}^\bullet$  to benzene yields hydroxycyclohexadienyl radical, which undergoes further reactions to form stable products, such as phenol.<sup>12,14-17</sup> In addition to ring attack, alkyl functional groups on aromatic compounds can be oxidized by  $\text{HO}^\bullet$ .<sup>18-20</sup> Most water treatment researchers and practitioners assume that the compounds mainly undergo sequential hydroxylation to produce phenols and dihydroxybenzenes, followed by ring cleavage to produce organic acids prior to mineralization (Figure 1).<sup>21-26</sup>

Although the formation of the expected products of sequential hydroxylation during oxidative water treatment is well documented, researchers have observed the production of ring cleavage products early in the oxidative treatment process that cannot be explained by

the sequential hydroxylation pathway.<sup>8</sup> This finding is consistent with results of pulse radiolysis studies in which O<sub>2</sub> reacted with the hydroxycyclohexadienyl radical to form peroxy radicals that underwent rearrangement to produce 6-carbon ring cleavage products in addition to the hydroxylation product (i.e., phenol).<sup>15,27</sup> A similar phenomenon has been observed in the gaseous phase, with HO• attack followed by O<sub>2</sub> addition to alkylbenzenes producing bicyclic peroxy radicals that rearranged to produce aldehydes and other ring-cleavage products.<sup>19,28–32</sup>

The reaction of aromatic compounds with SO<sub>4</sub><sup>•-</sup>, which has not been as extensively studied as reactions involving HO•, is thought to favor an electron transfer mechanism over H-abstraction, which forms the hydroxycyclohexadienyl radical as a result of a rapid reaction of the radical cation with water.<sup>33</sup> Sulfate radical addition also has been reported, although addition is considered to be quickly followed by an elimination step.<sup>34–36</sup> For substituted aromatic compounds, electron-withdrawing substituents greatly decrease the rate constant of SO<sub>4</sub><sup>•-</sup> reactions, whereas electron-donating substituents (e.g., alkyl groups) result in a slight increase in rate constants or have little effect.<sup>14,33</sup> In a previous study,<sup>8</sup> we observed a direct ring cleavage pathway following SO<sub>4</sub><sup>•-</sup> reactions with benzene, which resulted in the formation of a product identified as a 6 carbon-containing α,β-unsaturated aldehyde. Although the product was analyzed by nuclear magnetic resonance (NMR) spectroscopy and mass spectrometry (MS), the exact structure of the compound and the reaction mechanism could not be fully elucidated.

To provide insight into the formation of ring cleavage products during the initial stage of oxidation of alkyl-substituted aromatic contaminants, the reactions of HO• and SO<sub>4</sub><sup>•-</sup> with benzene and alkyl-substituted aromatic compounds (i.e., toluene, ethylbenzene and xylenes) were studied under conditions in which the majority of the dominant radical species (i.e., HO• and SO<sub>4</sub><sup>•-</sup>) should have reacted with the parent aromatic compound. By carefully tracking the fate of the aromatic compounds with a variety of sensitive analytical methods, it was possible to identify a suite of products, to assess the role of alkyl substituents on product distributions, and to provide a basis for predicting product distributions under conditions expected in oxidative water treatment systems.

## Materials and Methods

### Chemicals

Experiments were performed with analytical reagent grade benzene, toluene, ethylbenzene, and K<sub>2</sub>S<sub>2</sub>O<sub>8</sub> from Sigma-Aldrich (St. Louis, MO). Individually acquired chemicals were p-cresyl sulfate (98%) from APEX-BIO (Houston, TX), o-xylene (spectro grade) from J. T. Baker (Phillipsburg, NJ), and p-xylene from Eastman Kodak (Rochester, NY). m-Xylene and all other analytical reagents and standards were obtained from Fisher Scientific (Fairlawn, NJ). Solutions were prepared using 18.2 MΩ Milli-Q water from a Millipore system.

## Oxidation Experiments

Stock solutions of BTEX compounds were prepared in 100 mL volumetric flasks without headspace. For product analysis and quantification, initial concentrations of 1 mM aromatic compound and 10 mM oxidant were buffered at pH 8 with 50 mM borate.  $\text{H}_2\text{O}_2$  and  $\text{S}_2\text{O}_8^{2-}$  were activated by exposing samples in 8 mL quartz test tubes with no headspace to ultraviolet (UV) light from a 450-W medium pressure mercury lamp. For experiments with  $\text{H}_2\text{O}_2$ , the lamp was sleeved in a quartz immersion well and duplicate samples were collected every two minutes for a total of 30 minutes. A borosilicate immersion well was used for experiments with  $\text{S}_2\text{O}_8^{2-}$ , with samples collected at 20-min intervals for a total of 220 min. After collection, samples were immediately submerged in an ice bath and then stored at 4 °C until analysis, which occurred within 6 hours. To balance the need to produce sufficient amounts of products against the need to avoid the formation of products of a second radical attack on the parent compound, triplicate samples were collected when 30% loss of the parent compound was observed.

Control experiments in duplicate, consisting of buffered samples to which neither  $\text{H}_2\text{O}_2$  nor  $\text{S}_2\text{O}_8^{2-}$  were added, were conducted in tandem with the oxidation reactions. Less than 5% of the aromatic compounds were lost through direct UV photolysis, volatilization, or adsorption on the walls of the container, and this loss was accounted for in the mass balance calculations.

To assess the effect of dissolved  $\text{O}_2$  on product distribution, some experiments were conducted under a nitrogen atmosphere. A 50 mM borate buffer solution was deoxygenated by bubbling with nitrogen for 30 min, introduced to a glovebox, and allowed to equilibrate for 24 hours to remove any remaining dissolved oxygen. A solution of 1 mM toluene and 10 mM  $\text{K}_2\text{S}_2\text{O}_8$  was prepared in the buffer, sealed in 13 mL borosilicate vials, and irradiated under UV light alongside an identical sample prepared with an air-saturated solution. Triplicate samples were collected every 20 minutes and analyzed for transformation products.

## Analysis of Organic Compounds

Aromatic compounds and transformation products were analyzed with high performance liquid chromatography, using an Agilent 1260 HPLC system equipped with a UV/Vis Diode array detector (HPLC-UV/Vis). Parent compounds and aromatic products were quantified on a Waters Symmetry-C18 column with a 10 mM formic acid and acetonitrile gradient at 1.0 mL/min with HPLC-UV/Vis (Table S1). Formic acid was quantified using a Bio-Rad Aminex HPX-87H column and a 2.5 mM  $\text{H}_2\text{SO}_4$ /acetonitrile mixture at 0.4 mL/min and 60 °C. For the analysis of organic acids using this method,  $\text{H}_2\text{O}_2$  was quenched by addition of excess HOCl (i.e., 12 mM) prior to analysis, to reduce baseline noise.<sup>37</sup> Formaldehyde and acetaldehyde were derivatized with p-toluenesulfonylhydrazine (TSH) and analyzed via HPLC/MS-MS with a Phenomenex Synergi Hydro-RP column on an Agilent 1200 series HPLC system coupled to a 6460 triple quadrupole mass spectrometer (Text S1).<sup>38</sup> Parent compounds were measured immediately after sampling and transformation products were analyzed within 24 hours. Samples were refrigerated at 4 °C prior to injection.

The identification of unknown compounds was investigated with LC-MS/MS. HPLC was performed using a Hydro-RP column with the chromatographic method described in Text S1. Targeted analysis of unidentified aldehyde or ketone transformation products was accomplished by derivatization of the sample with TSH, which reacts with carbonyl groups but not carboxylic acids, followed by LC-MS/MS precursor ion scans for  $m/z$  139, a signature TSH fragment ion (Text S2).

Aromatic sulfate adducts for benzene, toluene, and ethylbenzene were quantified with a *p*-cresyl sulfate standard using the LC-MS/MS. Accurate masses and fragmentation patterns of unknown transformation products of toluene, ethylbenzene, and *o*-, *m*-, and *p*-xylene were obtained through high resolution mass spectrometry with a Thermo Scientific LTQ Orbitrap XL coupled to an Agilent 1260 HPLC system. Chromatographic separation for LC-MS/MS analysis of these sulfate adducts and unknown products was achieved with a Phenomenex Synergi Hydro-RP column with a flow rate of 0.4 mL/min, temperature of 25 °C, and injection volume of 25  $\mu$ L. Eluents were changed according to a gradient program that blended 10 mM formic acid (A) with methanol (B). The percentage of A was set at: 0 min, 100%; 3 min, 100%, 10 min, 70%; 30 min, 30%; 31.1 min, 100%; 35 min, 100%. The Orbitrap was operated in negative electrospray ionization (ESI) mode and MS<sup>2</sup> spectra were collected with High Energy Collisional Dissociation (HCD) at a collision energy of 35%.

### Compound Identification by Nuclear Magnetic Resonance (NMR) Spectroscopy

Unknown transformation products of BTEX compounds were further identified through NMR spectroscopy with a Bruker Avance 700 MHz instrument. Solid-phase extraction (SPE) was used to concentrate the products prior to NMR analysis. Due to the difficulty with the instrument lock and shim when deuterated organic solvents were used to wash the SPE column, likely from interference by the leaching of cartridge packing material, D<sub>2</sub>O (99.9 atom% D) was used as the NMR solvent. To produce a greater mass of the transformation product, additional experiments were performed with parent compound concentrations at the limit of solubility for the BTEX compounds. To this end, 175- $\mu$ L aliquots of individual compounds were added to 10 mM K<sub>2</sub>S<sub>2</sub>O<sub>8</sub> and 50 mM borate buffer in 150 mL borosilicate bottles and irradiated with UV light for 30 minutes. The SPE procedure for benzene, which was previously reported,<sup>8</sup> employed BondElut C18 cartridges pre-conditioned with water adjusted to pH 2 with HCl. For toluene and ethylbenzene, Oasis HLB 150 mg cartridges were conditioned with 30 mL of a 0.01 M HCl solution. 150 mL of sample was adjusted to pH 2 with HCl, then loaded onto one SPE column. In order to raise the pH above the pK<sub>a</sub> of the unidentified products, the column was washed with 0.4 mL of H<sub>2</sub>O at pH 9 (adjusted with NaOH), which raised the pH of the eluate to approximately 7. The unknown products were then eluted with 4 mL of neutral H<sub>2</sub>O. Finally, the cartridge was washed with 5 mL of methanol, which desorbed the aromatic compounds. This procedure yielded an enrichment factor of 1000 from an initial 2 L of solution. To concentrate the products for NMR, the eluate fractions in H<sub>2</sub>O were loaded onto the column by the same procedure, and the column was rinsed with 0.4 mL of D<sub>2</sub>O adjusted to pH 11 with NaOD (99+ atom % D). The compounds were then eluted out with 2 mL of D<sub>2</sub>O and evaporated under nitrogen to a final volume of 0.8 mL.

Quantitative NMR was used to determine the concentration of the investigated unknown products of benzene, toluene, and ethylbenzene. Signals were compared to an internal standard of maleic acid (Sigma-Aldrich standard for quantitative NMR, TraceCERT) and mass was calculated with the equation:

$$m(x) = m(std) \cdot \frac{MW(x)}{MW(std)} \cdot \frac{nH(std)}{nH(x)} \cdot \frac{A(x)}{A(std)} \quad (1)$$

where  $m(x)$  and  $m(std)$  are the masses of the unknown product and the standard,  $MW(x)$  and  $MW(std)$  are the molecular weights,  $nH(std)$  and  $nH(x)$  are the number of protons contributing to each signal, and  $A(x)$  and  $A(std)$  are the integrals of the signals.<sup>39</sup> Directly following NMR, a HPLC-UV/Vis calibration curve was prepared from the sample. These calibration curves for the unknown benzene, toluene, and ethylbenzene products were used for subsequent quantification in all respective samples.

## Results and Discussion

### Initial Oxidation of Aromatic Compounds

To separate the products of the first attack of  $\text{HO}^\bullet$  or  $\text{SO}_4^{\bullet-}$  on the aromatic compounds from transformation products produced by sequential oxidation of the ring, the initial concentration of the aromatic compound was ten times higher than the total amount of  $\text{HO}^\bullet$  or  $\text{SO}_4^{\bullet-}$  produced by photolytic or thermal activation. Under these conditions, oxidation of benzene by  $\text{HO}^\bullet$  or  $\text{SO}_4^{\bullet-}$  resulted in the formation of phenol, hydroquinone, catechol, benzoquinone, small organic acids (e.g., formate, acetate), acetaldehyde, and at least one other product (Figure 2). The yield of phenol, a product of a single radical attack, was only 24–36%, while hydroquinone, catechol and benzoquinone—products of the attack of a second radical on one of the initial reaction products—accounted for less than 9% of the total product yield (see Table S4). These findings were consistent with our prior study<sup>8</sup> in which phenol accounted for 34–57% of the benzene that was transformed when  $\text{SO}_4^{\bullet-}$  was generated by decomposition of  $\text{S}_2\text{O}_8^{2-}$  on mineral surfaces.

The compound that we had previously concluded to be a 6 carbon-containing  $\alpha,\beta$ -unsaturated aldehyde, which we refer to by the mass of its transformation product (TP126), was observed in experiments conducted with both  $\text{H}_2\text{O}_2$  and  $\text{S}_2\text{O}_8^{2-}$  (Figure 3). The molecular formula of TP126 was previously determined by QTOF-MS, which produced an accurate mass of  $m/z$  125.0246 as well as a fragmentation pattern.<sup>8</sup> TP126 also exhibited a characteristic UV absorption maximum at 352 nm (Figure S2).

Prior to analyzing TP126 by NMR, solid-phase extraction was used to separate the ring cleavage products from the parent compounds and other transformation products. When the solution pH was acidified to pH 2, all of the compounds were retained on the SPE column. When 4 mL of a pH 7 solution of water was passed through the SPE column, TP126 was eluted while the aromatic compounds remained on the column. This behavior suggests that the  $\text{pK}_a$  of TP126 was below 7, which is low for an acidic  $\alpha$ -hydrogen of a carbonyl but representative of a 1,3-diketone (e.g., the typical  $\alpha$ -hydrogen  $\text{pK}_a$  is 17 for aldehydes and 6–9 for 1,3-diketones).<sup>40,41</sup>



Our previous attempt to identify the unknown oxidation product formed when  $\text{SO}_4^{\bullet-}$  reacted with benzene indicated that the compound had a molecular formula of  $\text{C}_6\text{H}_6\text{O}_3$  and contained an  $\alpha,\beta$ -unsaturated aldehyde moiety. However, the exact structure of the compound was unclear from 1D  $^1\text{H}$  NMR and 2D  $^1\text{H}$ - $^1\text{H}$  NOESY due to an ambiguous signal at 8.95 ppm (Figure 4).<sup>8</sup> By employing 2D  $^1\text{H}$ - $^{13}\text{C}$  HSQC NMR with a DEPT135 pulse to differentiate between primary, secondary, and tertiary carbons, we were able to assign the terminal carbon as a  $-\text{CH}$  group due to the existence of a positive signal (Figure S3). Although the observed proton shift at 8.95 ppm and the observed carbon shift at 193 ppm were lower than values typically observed for aldehydes, it was within the range reported for compounds with 1,3-diketone groups, which exhibit electron delocalization through keto-enol tautomerization.<sup>42,43</sup> In the  $\text{D}_2\text{O}$  NMR solvent, the acidic  $\alpha$ -hydrogens exchanged with the solvent to produce either a broad undefined signal, or they produced a shift around 4.7 ppm that was masked by the residual solvent peak. As mentioned previously, the relatively low  $\text{pK}_a$  of this 1,3-diketo group was likely responsible for the pH-dependent retention of the product on the SPE column. In the aquatic environment, the keto tautomer is expected to co-exist in equilibrium with the enol due to the additional stability provided by hydrogen bonding in a polar solvent.<sup>44</sup> For example, 80% of acetylacetone persists in the keto form under aqueous conditions.<sup>41</sup> There was no evidence of an OH group around 16–17 ppm for enol tautomer when an NMR spectrum was obtained in  $\text{CD}_3\text{CN}$ , however, this does not rule out the possibility, as there may be rapid intramolecular H-exchange or a deprotonated group (Figure S3).<sup>45</sup> TP126 is depicted as a diketo tautomer in this study, with the acknowledgement that the trans-diketo conformation is the most stable, but is understood to co-exist in an equilibrium with the enol tautomer which is subject to temperature, pH, and solvent (Table S2).

Due to the difficulty in obtaining sufficient mass of the product for NMR analysis and the lower yield of this compound with  $\text{HO}^\bullet$  compared to  $\text{SO}_4^{\bullet-}$ , definitive NMR data were not obtained for the transformation of benzene when photolysis of  $\text{H}_2\text{O}_2$  was employed as the radical source. However, as depicted in Figure S2C,  $\text{MS}^2$  fragmentation patterns, high-resolution masses, and UV spectra were identical for TP126 when formed from  $\text{HO}^\bullet$  or  $\text{SO}_4^{\bullet-}$ . Retention times varied slightly between  $\text{HO}^\bullet$  and  $\text{SO}_4^{\bullet-}$  experiments when samples were analyzed by HPLC-UV/Vis with 100%  $\text{H}_2\text{O}$  as a mobile phase in order to reduce the effect of organic solvents on keto-enol tautomerization. The products of  $\text{HO}^\bullet$  and  $\text{SO}_4^{\bullet-}$  oxidation are likely stereoisomers with different orientations that affected their chromatographic separation.

These data suggest that TP126 is 4-oxo-2-hexenedial, a compound that has not been previously observed as a transformation product of benzene in oxidative water treatment or gaseous phase oxidation processes. A few studies, conducted prior to modern analytical techniques, had tentatively assigned products with similar UV absorption spectra as hydroxymuconaldehydes.<sup>46–49</sup> Structurally similar unsaturated 1,4-oxo- and hydroxy-enals are 4-oxo-2-nonenal (ONE) and 4-hydroxy-2-nonenal (HNE), have been studied extensively by toxicologists due to their association with oxidative stress and modification of DNA and proteins.<sup>50–52</sup>



The products of the initial oxidation of toluene and ethylbenzene oxidation followed a similar pattern to that observed for benzene, with the formation of transformation products resulting from hydroxylation of the ring *ortho* or *para* to the alkyl substituent, as well as ring cleavage to produce formic acid, formaldehyde, and other low molecular weight products (Figure 3B and 3C). In addition, products of oxidation of the alkyl side-chain (e.g., benzaldehyde, acetophenone) were detected. Ring cleavage products containing seven (TP140) or eight (TP154) carbons were isolated after reaction of toluene and ethylbenzene, respectively, by both HO<sup>•</sup> and SO<sub>4</sub><sup>•-</sup>. Similar to TP126, UV/Vis spectra of these transformation products showed absorption peaks around 352 nm (Figure S2) and LC-HRMS fragments that were consistent with the presence of methyl and ethyl groups on the parent compound (Figure S1). Two isomers were observed for toluene and for ethylbenzene when a chromatographic method different from that in Figure 3 was employed during analysis by LC-HRMS (Figure S1), indicating two different locations for ring cleavage.

For toluene, the <sup>1</sup>H NMR of the two unknown TP140 isomers formed upon reaction with SO<sub>4</sub><sup>•-</sup>, measured after SPE cleanup, was not as simple as that obtained for benzene due to the presence of multiple aromatic products that exhibited peaks from 7.1 to 7.7 ppm. The aldehydic shifts at 9.49 and 9.16 ppm, with coupling in the <sup>1</sup>H-<sup>1</sup>H COSY, suggested that one of the compounds is a dial (Figure S4). The methyl group at 2.36 ppm (Figure 4B inset) was downshifted by an additional neighboring carbonyl at C-3. For alkenes, a coupling constant (J) of 10 Hz is indicative of a *cis* conformation while J = 15 Hz implicates a *trans* conformation. This suggested a *cis* conformation for H-5 and H-4 and with H-3 being located *trans* to H-4. The other isomer, which lacked a signal in the typical aldehyde range, exhibited a signal at 8.87 ppm, which can be attributed to upshifting from a 1,3-diketone group similar to that observed for the benzene transformation product TP126. The absence of the α-H peaks of the diketo group in this enal isomer either indicates a fast exchange of these acidic protons with the solvent or signals identical to that of the residual water peak. On the basis of these data, we conclude that the two TP140 isomers were most likely C<sub>7</sub> ring cleavage products: 5-methyl-4-oxo-2-hexenedial and 3,6-dioxo-4-heptenal. In experiments with H<sub>2</sub>O<sub>2</sub>, the TP140 isomers also were observed by HPLC-UV/Vis and in mass spectra, but were not produced in high enough yields to allow for structural analysis by NMR (Figure S2C).

The unknown ring-cleavage product of SO<sub>4</sub><sup>•-</sup> attack on ethylbenzene (TP154) exhibited a relatively simple <sup>1</sup>H NMR spectrum after SPE separation from the other products (Figure 4C). Similarities between the ethylbenzene transformation products and those of toluene were evident. The dial isomer contained signals at 9.52 and 9.18 ppm, likely attributable to aldehydes. The unsubstituted 1,3-diketone in the enal isomer exhibited upshifting of the aldehyde moiety to 8.88 ppm. A positive peak from <sup>1</sup>H-<sup>13</sup>C HSQC-DEPT135 for ethylbenzene confirmed this signal to be a terminal -CH (Figure S5). Coupling constants were consistent with the *cis* conformation of H-5 and H-4 and the *trans* conformation of H-4 and H-3. On the basis of these data, we conclude that TP154 most likely consisted of two C<sub>8</sub> isomers: 5-ethyl-4-oxo-2-hexenedial and 3,6-dioxo-4-octenal. As was the case with benzene and ethylbenzene oxidized by H<sub>2</sub>O<sub>2</sub>, TP154 was observed by HPLC/UV and in mass spectra, but was not produced in high enough yields to allow for structural analysis by NMR by the same method.

The situation was more complicated for the xylene isomers. HPLC-UV/Vis chromatograms lacked baseline-resolved peaks with absorption bands similar to TP154 around 280 and 350 nm. Analysis by LC-HRMS revealed products with exact masses of  $m/z = 153.0553$  for all of the xylenes, suggesting structures similar to that of the ethylbenzene ring cleavage products, albeit with two methyls instead of a single ethyl group (Figure S6). Based on the peak areas from LC-MS/MS, concentrations of these products were much lower than TP154 and thus NMR was not attempted. Either the analogous ring cleavage pathway for o-, m-, and p-xylene produces  $C_8H_{10}O_3$  products with different structures and UV absorption spectra, or this side reaction is unlikely and yields are extremely low.

In addition to the transformation products discussed above, reaction of  $SO_4^{\bullet-}$  with benzene, toluene and ethylbenzene also led to the formation of transformation products that contained a sulfate group on the aromatic ring (Figure 5C and Figure S7). Organosulfates including phenyl sulfate, p-cresyl sulfate, p-ethylphenyl sulfate, and o-methylbenzyl sulfate are urinary metabolites of BTEX compounds<sup>53</sup> but have not previously been reported during oxidative water treatment with  $SO_4^{\bullet-}$ . For toluene, the putative organosulfate compound was confirmed to be cresyl sulfate through comparison of the mass spectrum and HPLC retention time with that of an authentic standard of p-cresyl sulfate (Figure S7). The other compounds exhibited similar fragmentation patterns (loss of  $SO_3$ ) to that of p-cresyl sulfate with additional methyl or ethyl groups (Table S3). These findings are consistent with previous data indicating that in addition to electron transfer,  $SO_4^{\bullet-}$  reactions can result in sulfate addition to aromatic rings as a minor pathway.<sup>33–36</sup> For the alkyl-substituted aromatic compounds, three peaks of the same mass were observed at around the same retention time, indicating that sulfate addition occurred at multiple sites (Figure S7).

Photolysis of  $S_2O_8^{2-}$  in nitrogen-purged solutions resulted in much higher yields of the sulfate-containing product of toluene and lower yields of TP140 (i.e., the 7-carbon containing ring cleavage products) than in samples in which  $O_2$  was present (Figure 5). These experiments indicate that  $SO_4^{\bullet-}$  addition is the first step in the ring cleavage mechanism that yields carbon chain-retaining aldehydes and that  $O_2$  plays an important role in the subsequent steps in the process. Ring-opened organosulfate intermediates were not observed on the time scale of analysis and further research is required to determine whether the sulfate group is eliminated or hydrolyzed prior to or after ring cleavage, or whether it plays a role in the ring opening mechanism.

### Product Distribution

To determine the relative importance of the different transformation products, we quantified the loss of the parent compound and the production of transformation products (Figure 6, Table S4). In the initial stages of the reaction (when around 30% of the parent compound had been lost), the products of ring hydroxylation and alkyl-substituent oxidation, expressed in terms of the number of moles of carbon, accounted for between 12 and 38% of the reacted carbon. Hydroxylation of the ring was highest for benzene (i.e., 33 to 36% of all products quantified) whereas oxidation of the alkyl substituent accounted for most of the detected products when ethylbenzene reacted with  $SO_4^{\bullet-}$ . The contribution from aromatic organosulfates was significant for the alkylbenzenes: for toluene and ethylbenzene, the

sulfate adduct accounted for 12–13% of the mass of reacted parent compound when  $\text{SO}_4^{\bullet-}$  initiated the oxidation process. Only a 2–3% yield of phenyl sulfate was found for benzene. Stabilization of the radical by the alkyl substituent may account for this difference.

Ring cleavage products that were amenable to quantification accounted for 2–10% of the reacted carbon. The reactions were monitored until around 70% loss of the parent compounds, with little change in the relative distribution of the transformation products. Acetaldehyde accounted for 1–3% of the reacted carbon for all three compounds, with similar concentrations for both radical species. Formic acid accounted for 3–7% of the reacted mass in experiments conducted with  $\text{HO}^\bullet$ . In addition to these prominent products, other organic acids (acetic acid, maleic acid, and fumaric acid) and aldehydes (formaldehyde, glyoxal, methylglyoxal and 2-butene-1,4-dial) were detected in all of the reactions. Concentrations accounted for roughly 0.1% of the reacted mass and thus quantification was not optimized and is not reported in this study. The 6, 7 and 8-carbon ring cleavage products (i.e., TP126, TP140 and TP154) accounted for 0.1 to 0.4% of the reacted carbon, with concentrations that were approximately twice as high when  $\text{SO}_4^{\bullet-}$  initiated the oxidation process relative to reactions initiated by  $\text{HO}^\bullet$ . The maximum yields of the 6, 7 and 8-carbon transformation products, corresponding to 0.5–1% of the mass of carbon lost, were observed when around half of the parent compound had been lost.

Although these results represent the most comprehensive effort to detect the products of oxidation of aromatic compounds by these two radicals, we were unable to account for 57–85% of the reacted carbon. One likely source of the missing mass of carbon are ring cleavage products which could not be quantified by the used methods. Samples derivatized with TSH and analyzed with TSH-targeted precursor ion scans in LC-MS/MS (Figure S8) and the HPLC-UV/Vis (Figure S9) method used for quantification of organic acids revealed the presence of 10 to 20 peaks that could not be attributed to the low molecular weight compounds for which standards were available. It is likely that further oxidation of the 6, 7 and 8-carbon unsaturated aldehyde products (i.e., TP126, TP140 and TP154) results in the analogous carboxylic acids or further cleavage into smaller acids. Another possibility is mineralization of the aromatic compounds (i.e., formation of  $\text{CO}_2$ ), which could have occurred through various decarboxylation reactions during the ring cleavage process. Finally, it is possible that the organic peroxy radical reacted with benzene to produce dimers and other high molecular weight species that were not amenable to analysis.<sup>54</sup> Additional research is needed to identify and quantify the compounds observed by LC-MS/MS and assess the importance of mineralization and polymerization as sinks for the reacted carbon.

### **Oxidation of Benzene and Alkyl-Substituted Aromatic Compounds by $\text{HO}^\bullet$ and $\text{SO}_4^{\bullet-}$**

Formation of phenolic compounds and ring cleavage products after the attack of only one  $\text{SO}_4^{\bullet-}$  or  $\text{HO}^\bullet$  on the aromatic compound indicates that the hydroxycyclohexadienyl radical (i.e., the species that is common to both  $\text{HO}^\bullet$  and  $\text{SO}_4^{\bullet-}$  reactions) can undergo several different side reactions that produce an array of transformation products. In air-saturated solutions, hydroxycyclohexadienyl radicals react with dissolved  $\text{O}_2$  to produce hydroxycyclohexadienylperoxy radicals.<sup>15</sup> These species can eliminate  $\text{HO}_2^\bullet$  to produce hydroxylated products (Figure 3).<sup>12,14,54</sup> In an alternative pathway, they can also undergo an

intramolecular addition to a double bond to form a bicyclic peroxy radical, which may then react further with O<sub>2</sub> (Figure 7). If there are no oxidants present that can undergo one-electron reactions, the bicyclic peroxy radical may disproportionate to produce two endoperoxides. Both of these products are unstable and can undergo ring scission, with one of them eliminating carbon monoxide to produce five- and six-membered unsaturated aldehydes and ketones.<sup>15</sup> In the gaseous phase, the bicyclic peroxy radical reacts with NO<sub>x</sub>, which promotes ring cleavage and results in the radical being quenched.<sup>29,31,55–58</sup> In the aqueous phase, it is also possible that the bicyclic peroxy radical undergoes rearrangement and electron transfer reactions that propagate the radical chain reaction and generate other products.

Consistent with our results, Pan et al. (1993), who generated HO• by pulse radiolysis at high benzene concentrations in an unbuffered system, observed phenol yields of approximately 53% and ring cleavage products which accounted for approximately 35% of the carbon that was initially present.<sup>15</sup> Using ion chromatography for organic acids and trimethylsilane derivitization after borohydride reduction prior to GC-MS to detect aldehydes, ketones, and alcohols, they observed formic acid, formaldehyde, acetaldehyde, and 15 additional three to six-carbon compounds containing aldehydes, ketone, alcohols, and carboxylic acid functional groups. On the basis of the mass spectra, they classified the most prominent of the six-carbon containing ring cleavage products as 2,5-dihydroxy-3-hexenedial, (C<sub>6</sub>H<sub>8</sub>O<sub>4</sub>). This compound is similar to the major product of benzene oxidation that we detected (C<sub>6</sub>H<sub>6</sub>O<sub>3</sub>). It is possible that both compounds were produced but that they were only detected by the specific analytical approach employed in each study.

The reactions of alkyl-substituted aromatic compounds proved additional insight into the reaction mechanism. For toluene and ethylbenzene, the presence of two different isomers of the 7- and 8-membered ring cleavage products suggests that there are multiple pathways of O<sub>2</sub> addition and ring cleavage. Researchers have postulated mechanisms that can account for the production of ring cleavage products at a single site to form muconaldehyde-like products including: 1) β-fragmentation of a hydroxycyclohexadienyl oxyl radical<sup>59</sup> or 1,2-peroxy radical<sup>60</sup> to open the ring, followed by further O<sub>2</sub>/HO<sub>2</sub>• addition/elimination reactions; and, 2) a gas phase NO-free pathway involving O<sub>2</sub> that forms an epoxy muconaldehyde.<sup>61,62</sup> A unimolecular rearrangement comprising of C<sub>α</sub>-O bond cleavage and β-H migration has been proposed to explain the formation of 1,3-diketones from α,β-epoxy ketone radical ions.<sup>63</sup> Further research and computational work are required to improve understanding of the specific pathways of ring cleavage.

## Environmental Implications

Radical oxidation of aromatic compounds involve numerous competing side reactions that produce a wide array of products (Figure 2). As soon as radicals react with aromatic compounds, a cascade of reactions occurs than can result in the formation of ring cleavage products and low molecular weight oxygenated compounds. Some of these compounds are readily metabolized *in vivo* or are degraded by bacteria (e.g., organic acids, acetaldehyde). Other compounds (e.g., α,β-unsaturated aldehydes and ketones, 1,3-dicarbonyls) are strong electrophiles that could be of concern for human health.<sup>50,51</sup> Despite their low yields, α,β-

unsaturated aldehydes are of concern due to their relatively high toxicity.<sup>51</sup> Based on the results reported here as well as our previous study of HO• oxidation of phenolic compounds, the ring cleavage mechanisms that produce  $\alpha,\beta$ -unsaturated aldehydes appear to be a common feature of radical oxidation of phenols and alkylated aromatic compounds.<sup>64</sup> We did not observe this mechanism in preliminary experiments with nitroaromatics or in chlorobenzenes but on the basis of the results reported here, we suspect that radical reactions may also produce ring cleavage products in conjugated ring systems (e.g., PAHs) and in natural organic matter through an analogous mechanism. In addition, the formation of  $\alpha,\beta$ -unsaturated aldehydes has been recently observed for the reaction of phenols with HOCl,<sup>65</sup> thus indicating that the formation of these compounds might be much more common than previously known.

Numerous competing ring cleavage pathways resulting in a suite of both saturated and  $\alpha,\beta$ -unsaturated aldehydes, each accounting for roughly 1% of the reacted carbon mass, could have significant implications for treated water due to their relatively high toxicity.<sup>50,66</sup> Due to the difficulty in classifying the product distribution for the array of aromatic compounds that may undergo these reactions as well as the challenge of quantifying them at low concentrations, *in vitro* toxicity assays and bioanalytical approaches that investigate their interactions with biomolecules<sup>64,65</sup> could be a useful tools to assess the formation of  $\alpha,\beta$ -unsaturated carbonyls and other reactive electrophiles produced by aromatic contaminant oxidation by radicals used in water treatment.

## Supplementary Material

Refer to Web version on PubMed Central for supplementary material.

## Acknowledgements

This research was supported by the US National Institute for Environmental Health Sciences Superfund Research Program (Grant P42 ES004705) at the University of California, Berkeley.

## References

- (1). Tsitonaki A; Petri BG; Crimi M; Mosbk H; Siegrist RL; Bjerg PL In Situ Chemical Oxidation of Contaminated Soil and Groundwater Using Persulfate: A Review. *Crit. Rev. Environ. Sci. Technol* 2010, 40 (1), 55–91. 10.1080/10643380802039303.
- (2). Anipsitakis GP; Dionysiou DD Transition Metal/UV-Based Advanced Oxidation Technologies for Water Decontamination. *Appl. Catal. B Environ* 2004, 54 (3), 155–163. 10.1016/j.apcatb.2004.05.025.
- (3). Ike IA; Linden KG; Orbell JD; Duke M Critical Review of the Science and Sustainability of Persulphate Advanced Oxidation Processes. *Chem. Eng. J* 2018, 338, 651–669. 10.1016/j.cej.2018.01.034.
- (4). Waclawek S; Lutze HV; Grübel K; Padil VVT; erník M; Dionysiou DD Chemistry of Persulfates in Water and Wastewater Treatment: A Review. *Chem. Eng. J* 2017, 330, 44–62. 10.1016/j.cej.2017.07.132.
- (5). Krembs FJ; Siegrist RL; Crimi M; Furrer RF; Petri BG ISCO for Groundwater Remediation: Analysis of Field Applications and Performance. *Ground Water Monit. Remediat* 2010, 30 (4), 42–53. 10.1111/j.1745-6592.2010.01312.x.

- (6). Pham AL; Doyle FM; Sedlak DL Kinetics and Efficiency of H<sub>2</sub>O<sub>2</sub> Activation by Iron-Containing Minerals and Aquifer Materials. *Water Res.* 2012, 46 (19), 6454–6462. 10.1016/j.watres.2012.09.020. [PubMed: 23047055]
- (7). Liu H; Bruton TA; Doyle FM; Sedlak DL In Situ Chemical Oxidation of Contaminated Groundwater by Persulfate: Decomposition by Fe(III)- and Mn(IV)-Containing Oxides and Aquifer Materials. *Environ. Sci. Technol* 2014, 48 (17), 10330–10336. 10.1021/es502056d. [PubMed: 25133603]
- (8). Liu H; Bruton TA; Li W; Van Buren J; Prasse C; Doyle FM; Sedlak DL Oxidation of Benzene by Persulfate in the Presence of Fe(III)- and Mn(IV)-Containing Oxides: Stoichiometric Efficiency and Transformation Products. *Environ. Sci. Technol* 2016, 50 (2), 890–898. 10.1021/acs.est.5b04815. [PubMed: 26687229]
- (9). Marron EL; Mitch WA; Gunten U. von; Sedlak DL A Tale of Two Treatments: The Multiple Barrier Approach to Removing Chemical Contaminants During Potable Water Reuse. *Acc. Chem. Res* 2019, 52 (3), 615–622. 10.1021/acs.accounts.8b00612. [PubMed: 30821146]
- (10). Siegrist RL; Crimi M; Brown RA In Situ Chemical Oxidation: Technology Description and Status In In Situ Chemical Oxidation for Groundwater Remediation; Siegrist RL, Crimi M,J,S, Eds.; Springer-Verlag: New York, NY, 2011; Vol. 3, pp 1–32. 10.1007/978-1-4419-7826-4.
- (11). Anbar M; Meyerstein D; Neta P The Reactivity of Aromatic Compounds toward Hydroxyl Radicals. *J. Phys. Chem* 1966, 70 (8), 2660–2662. 10.1021/j100880a034.
- (12). Dorfman LM; Taub IA; Bühler RE Pulse Radiolysis Studies. I. Transient Spectra and Reaction-Rate Constants in Irradiated Aqueous Solutions of Benzene. *J. Chem. Phys* 1962, 36 (11), 3051–3061. 10.1063/1.1732425.
- (13). Neta P; Dorfman LM Pulse Radiolysis Studies XIII. Rate Constants for the Reaction of Hydroxyl Radicals with Aromatic Compounds in Aqueous Solutions. In *Radiation Chemistry; Advances in Chemistry*; American Chemical Society, 1968; Vol. 81, pp 222–230. 10.1021/ba-1968-0081.ch015.
- (14). Fang X; Pan X; Rahmann A; Schuchmann H; von Sonntag C Reversibility in the Reaction of Cyclohexadienyl Radicals with Oxygen in Aqueous Solution. *Chem. Eur. J* 1995, 1 (7), 423–429. 10.1002/chem.19950010706.
- (15). Pan X-M; Schuchmann MN; von Sonntag C Oxidation of Benzene by the OH Radical. A Product and Pulse Radiolysis Study in Oxygenated Aqueous Solution. *J. Chem. Soc., Perkins Trans.* 2 1993, No. 3, 289–297. 10.1039/P29930000289.
- (16). Pan X-M; von Sonntag C OH-Radical-Induced Oxidation of Benzene in the Presence of Oxygen:  $R\cdot + O_2 \rightleftharpoons RO_2\cdot$  Equilibria in Aqueous Solution. A Pulse Radiolysis Study. *Zeitschrift für Naturforsch. B* 1990, 45 (9), 1337–1340. 10.1515/znb-1990-0920.
- (17). Steenken S Addition-Elimination Paths in Electron-Transfer Reactions between Radicals and Molecules. Oxidation of Organic Molecules by the OH Radical. *J. Chem. Soc., Faraday Trans.* 1 1987, 83 (1), 113–124. 10.1039/F19878300113.
- (18). Merz JH; Waters WA The Oxidation of Aromatic Compounds by Means of the Free Hydroxyl Radical. *J. Chem. Soc* 1949, 2427–2433. 10.1039/JR9490002427.
- (19). Birdsall AW; Andreoni JF; Elrod MJ Investigation of the Role of Bicyclic Peroxy Radicals in the Oxidation Mechanism of Toluene. *J. Phys. Chem. A* 2010, 114 (39), 10655–10663. 10.1021/jp105467e. [PubMed: 20836528]
- (20). Liu G; Ji J; Huang H; Xie R; Feng Q; Shu Y; Zhan Y; Fang R; He M; Liu SL; Ye XG; Leung DYC UV/H<sub>2</sub>O<sub>2</sub>: An Efficient Aqueous Advanced Oxidation Process for VOCs Removal. *Chem. Eng. J* 2017, 324, 44–50. 10.1016/j.cej.2017.04.105.
- (21). Gligorovski S; Strekowski R; Barbati S; Vione D Environmental Implications of Hydroxyl Radicals ( $\bullet$ OH). *Chem. Rev* 2015, 115 (24), 13051–13092. 10.1021/cr500310b. [PubMed: 26630000]
- (22). Long A; Lei Y; Zhang H Degradation of Toluene by a Selective Ferrous Ion Activated Persulfate Oxidation Process. *Ind. Eng. Chem. Res* 2014, 53 (3), 1033–1039. 10.1021/ie402633n.
- (23). Watts RJ; Teel AL Chemistry of Modified Fenton's Reagent (Catalyzed H<sub>2</sub>O<sub>2</sub> Propagations-CHP) for in Situ Soil and Groundwater Remediation. *J. Environ. Eng* 2005, 131 (4), 612–622. 10.1061/(ASCE)0733-9372(2005)131:4(612).



- (24). Zazo JA; Casas JA; Mohedano AF; Gilarranz MA; Rodríguez JJ Chemical Pathway and Kinetics of Phenol Oxidation by Fenton's Reagent. *Environ. Sci. Technol* 2005, 39 (23), 9295–9302. 10.1021/es050452h. [PubMed: 16382955]
- (25). Devlin HR; Harris IJ Mechanism of the Oxidation of Aqueous Phenol with Dissolved Oxygen. *Ind. Eng. Chem. Fundam* 1984, 23 (4), 387–392. 10.1021/i100016a002.
- (26). Scheck CK; Frimmel FH Degradation of Phenol and Salicylic Acid by Ultraviolet Radiation/Hydrogen Peroxide/Oxygen. *Water Res.* 1995, 29 (10), 2346–2352. 10.1016/0043-1354(95)00060-X.
- (27). von Sonntag C; Dowideit P; Fang X; Mertens R; Pan X; Schuchmann MN; Schuchmann H The Fate of Peroxyl Radicals in Aqueous Solution. *Water Sci. Technol* 1997, 35 (4), 9–15. 10.1016/S0273-1223(97)00003-6.
- (28). Elrod MJ Kinetics Study of the Aromatic Bicyclic Peroxy Radical + NO Reaction: Overall Rate Constant and Nitrate Product Yield Measurements. *J. Phys. Chem. A* 2011, 115 (28), 8125–8130. 10.1021/jp204308f. [PubMed: 21661722]
- (29). Wang S; Wu R; Berndt T; Ehn M; Wang L Formation of Highly Oxidized Radicals and Multifunctional Products from the Atmospheric Oxidation of Alkylbenzenes. *Environ. Sci. Technol* 2017, 51 (15), 8442–8449. 10.1021/acs.est.7b02374. [PubMed: 28682596]
- (30). Pan S; Wang L Atmospheric Oxidation Mechanism of m-Xylene Initiated by OH Radical. *J. Phys. Chem. A* 2014, 118 (45), 10778–10787. 10.1021/jp506815v. [PubMed: 25320837]
- (31). Wu R; Pan S; Li Y; Wang L Atmospheric Oxidation Mechanism of Toluene. *J. Phys. Chem. A* 2014, 118 (25), 4533–4547. 10.1021/jp500077f. [PubMed: 24901213]
- (32). Lay TH; Bozzelli JW; Seinfeld JH Atmospheric Photochemical Oxidation of Benzene: Benzene + OH and the Benzene-OH Adduct (Hydroxyl-2,4-Cyclohexadienyl) + O<sub>2</sub>. *J. Phys. Chem* 1996, 100 (16), 6543–6554. 10.1021/jp951726y.
- (33). Neta P; Madhavan V; Zemel H; Fessenden RW Rate Constants and Mechanism of Reaction of SO<sub>4</sub><sup>•-</sup> with Aromatic Compounds. *J. Am. Chem. Soc* 1977, 99 (1), 163–164. 10.1021/ja00443a030.
- (34). Merga G; Aravindakumar CT; Rao BSM; Mohan H; Mittal JP Pulse Radiolysis Study of the Reactions of SO<sub>4</sub><sup>•-</sup> with Some Substituted Benzenes in Aqueous Solution. *J. Chem. Soc., Faraday Trans* 1994, 90 (4), 597–604. 10.1039/FT9949000597.
- (35). Norman ROC; Storey PM; West PR Electron Spin Resonance Studies. Part XXV. Reactions of the Sulphate Radical Anion with Organic Compounds. *J. Chem. Soc. B* 1970, 1087–1095. 10.1039/J29700001087.
- (36). Steenken S One-Electron Redox Reactions between Radicals and Organic Molecules. An Addition/Elimination (Inner-Sphere) Path [1]. In *Electron Transfer II Topics in Current Chemistry*; Mattay J, Ed.; Springer, Berlin, Heidelberg, 1996; Vol. 177, pp 125–145. 10.1007/3-540-60110-4\_4.
- (37). Keen OS; Dotson AD; Linden KG Evaluation of Hydrogen Peroxide Chemical Quenching Agents Following an Advanced Oxidation Process. *J. Environ. Eng* 2013, 139 (1), 137–140. 10.1061/(ASCE)EE.1943-7870.0000619.
- (38). Siegel D; Meinema AC; Permentier H; Hopfgartner G; Bischoff R Integrated Quantification and Identification of Aldehydes and Ketones in Biological Samples. *Anal. Chem* 2014, 86 (10), 5089–5100. 10.1021/ac500810r. [PubMed: 24745975]
- (39). Rundlöf T; Mathiasson M; Bekiroglu S; Hakkarainen B; Bowden T; Arvidsson T Survey and Qualification of Internal Standards for Quantification by <sup>1</sup>H NMR Spectroscopy. *J. Pharm. Biomed. Anal* 2010, 52 (5), 645–651. 10.1016/j.jpba.2010.02.007. [PubMed: 20207092]
- (40). Bruice PY *Organic Chemistry*, 5th ed.; Prentice Hall: Upper Saddle River, NJ, 2006.
- (41). Bunting JW; Kanter JP; Nelander R; Wu Z The Acidity and Tautomerism of β-Diketones in Aqueous Solution. *Can. J. Chem* 1995, 73 (8), 1305–1311. 10.1139/v95-161.
- (42). George WO; Mansell VG Nuclear Magnetic Resonance Spectra of Acetylaldehyde and Malondialdehyde. *J. Chem. Soc. B* 1968, 132–134. 10.1039/J29680000132.
- (43). Koltsov AI Enol-Enol Tautomerism in Cis-Keto-Enols. *J. Mol. Struct* 1998, 444 (1–3), 1–11. 10.1016/S0022-2860(97)00261-5.



- (44). Kol'tsov AI; Kheifets GM Investigation of Keto–Enol Tautomerism by Nuclear Magnetic Resonance Spectroscopy. *Russ. Chem. Rev* 1971, 40 (9), 773–788. 10.1070/rc1971v040n09abeh001969.
- (45). Zawadiak J; Mrzyczek M UV Absorption and Keto-Enol Tautomerism Equilibrium of Methoxy and Dimethoxy 1,3-Diphenylpropane-1,3-Diones. *Spectrochim. Acta A Mol. Biomol. Spectrosc* 2010, 75 (2), 925–929. 10.1016/j.saa.2009.12.040. [PubMed: 20047853]
- (46). Goodman J; Steigman J Products of the Radiolysis of Water Containing Benzene and Air. *J. Phys. Chem* 1958, 62 (8), 1020–1022. 10.1021/j150566a037.
- (47). Srinivasan TKK; Balakrishnan I; Reddy MP On the Nature of the Products Gamma Radiolysis of Aerated Aqueous Solutions of Benzene. *J. Phys. Chem* 1969, 73 (6), 2071–2073. 10.1021/j100726a076.
- (48). Balakrishnan I; Reddy MP Effect of Temperature on the Gamma Radiolysis of Aqueous Solutions. *J. Phys. Chem* 1972, 76 (9), 1273–1279. 10.1021/j100653a008.
- (49). Zhihua Z; Goldstein BD; Witz G Iron-Stimulated Ring-Opening of Benzene in a Mouse Liver Microsomal System. *Biochem. Pharmacol* 1995, 50 (10), 1607–1617. 10.1016/0006-2952(95)02043-8. [PubMed: 7503763]
- (50). Guillén MD; Goicoechea E Toxic Oxygenated  $\alpha,\beta$ -Unsaturated Aldehydes and Their Study in Foods: A Review. *Crit. Rev. Food Sci. Nutr* 2008, 48 (2), 119–136. 10.1080/10408390601177613. [PubMed: 18274968]
- (51). Lopachin RM; Gavin T Molecular Mechanisms of Aldehyde Toxicity: A Chemical Perspective. *Chem. Res. Toxicol* 2014, 27 (7), 1081–1091. 10.1021/tx5001046. [PubMed: 24911545]
- (52). Galligan JJ; Rose KL; Beavers WN; Hill S; Tallman KA; Tansey WP; Marnett LJ Stable Histone Adduction by 4-Oxo-2-Nonenal: A Potential Link between Oxidative Stress and Epigenetics. *J. Am. Chem. Soc* 2014, 136 (34), 11864–11866. 10.1021/ja503604t. [PubMed: 25099620]
- (53). Ballet C; Correia MSP; Conway LP; Locher TL; Lehmann LC; Garg N; Vujasinovic M; Deindl S; Löhr J-M; Globisch D New Enzymatic and Mass Spectrometric Methodology for the Selective Investigation of Gut Microbiota-Derived Metabolites. *Chem. Sci* 2018, 9, 6233–6239. 10.1039/c8sc01502c. [PubMed: 30090311]
- (54). Al-Sheikhly M; Poster DL; An J-C; Neta P; Silverman J; Huie RE Ionizing Radiation-Induced Destruction of Benzene and Dienes in Aqueous Media. *Environ. Sci. Technol* 2006, 40 (9), 3082–3088. 10.1021/es052533j. [PubMed: 16719115]
- (55). Nakao S; Clark C; Tang P; Sato K; Cocker D Secondary Organic Aerosol Formation from Phenolic Compounds in the Absence of NO<sub>x</sub>. *Atmos. Chem. Phys* 2011, 11, 10649–10660. 10.5194/acp-11-10649-2011.
- (56). Barnes I Aromatic Hydrocarbons In *Encyclopedia of Atmospheric Sciences 2nd Edition*; North GR, Pyle JA, Zhang F, Eds.; Elsevier, 2015; Vol. 6, pp 243–250. 10.1016/B978-0-12-382225-3.00424-2.
- (57). Andino JM; Smith JN; Flagan RC; Goddard WA; Seinfeld JH Mechanism of Atmospheric Photooxidation of Aromatics: A Theoretical Study. *J. Phys. Chem* 1996, 100 (26), 10967–10980. 10.1021/jp952935l.
- (58). Baltaretu CO; Lichtman EI; Hadler AB; Elrod MJ Primary Atmospheric Oxidation Mechanism for Toluene. *J. Phys. Chem. A* 2009, 113 (1), 221–230. 10.1021/jp806841t. [PubMed: 19118482]
- (59). Ghigo G; Tonachini G From Benzene to Muconaldehyde: Theoretical Mechanistic Investigation on Some Tropospheric Oxidation Channels. *J. Am. Chem. Soc* 1999, 121 (36), 8366–8372. 10.1021/ja990552l.
- (60). Sato K; Takimoto K; Tsuda S Degradation of Aqueous Phenol Solution by Gamma Irradiation. *Environ. Sci. Technol* 1978, 12 (9), 1043–1046. 10.1021/es60145a016.
- (61). Motta F; Ghigo G; Tonachini G Oxidative Degradation of Benzene in the Troposphere. Theoretical Mechanistic Study of the Formation of Unsaturated Dialdehydes and Dialdehyde Epoxides. *J. Phys. Chem. A* 2002, 106 (17), 4411–4422. 10.1021/jp015619h.
- (62). Wang L; Wu R; Xu C Atmospheric Oxidation Mechanism of Benzene. Fates of Alkoxy Radical Intermediates and Revised Mechanism. *J. Phys. Chem. A* 2013, 117, 14163–14168. 10.1021/jp4101762. [PubMed: 24369824]

- (63). Hasegawa E; Ishiyama K; Horaguchi T; Shimizu T Exploratory Study on Photoinduced Single Electron Transfer Reactions of  $\alpha,\beta$ -Epoxy Ketones with Amines. *J. Org. Chem* 1991, 56 (4), 1631–1635. 10.1021/jo00004a052.
- (64). Prasse C; Ford B; Nomura DK; Sedlak DL Unexpected Transformation of Dissolved Phenols to Toxic Dicarbonyls by Hydroxyl Radicals and UV Light. *Proc. Natl. Acad. Sci* 2018, 115 (10), 2311–2316. 10.1073/pnas.1715821115. [PubMed: 29463747]
- (65). Prasse C; von Gunten U; Sedlak DL Chlorination of Phenols Revisited: Unexpected Formation of  $\alpha,\beta$ -Unsaturated C<sub>4</sub>-Dicarbonyl Ring Cleavage Products. *Environ. Sci. Technol* In review.
- (66). Szmigielski R Evidence for C<sub>5</sub> Organosulfur Secondary Organic Aerosol Components from In-Cloud Processing of Isoprene: Role of Reactive SO<sub>4</sub> and SO<sub>3</sub> Radicals. *Atmos. Environ* 2016, 130, 14–22. 10.1016/j.atmosenv.2015.10.072.

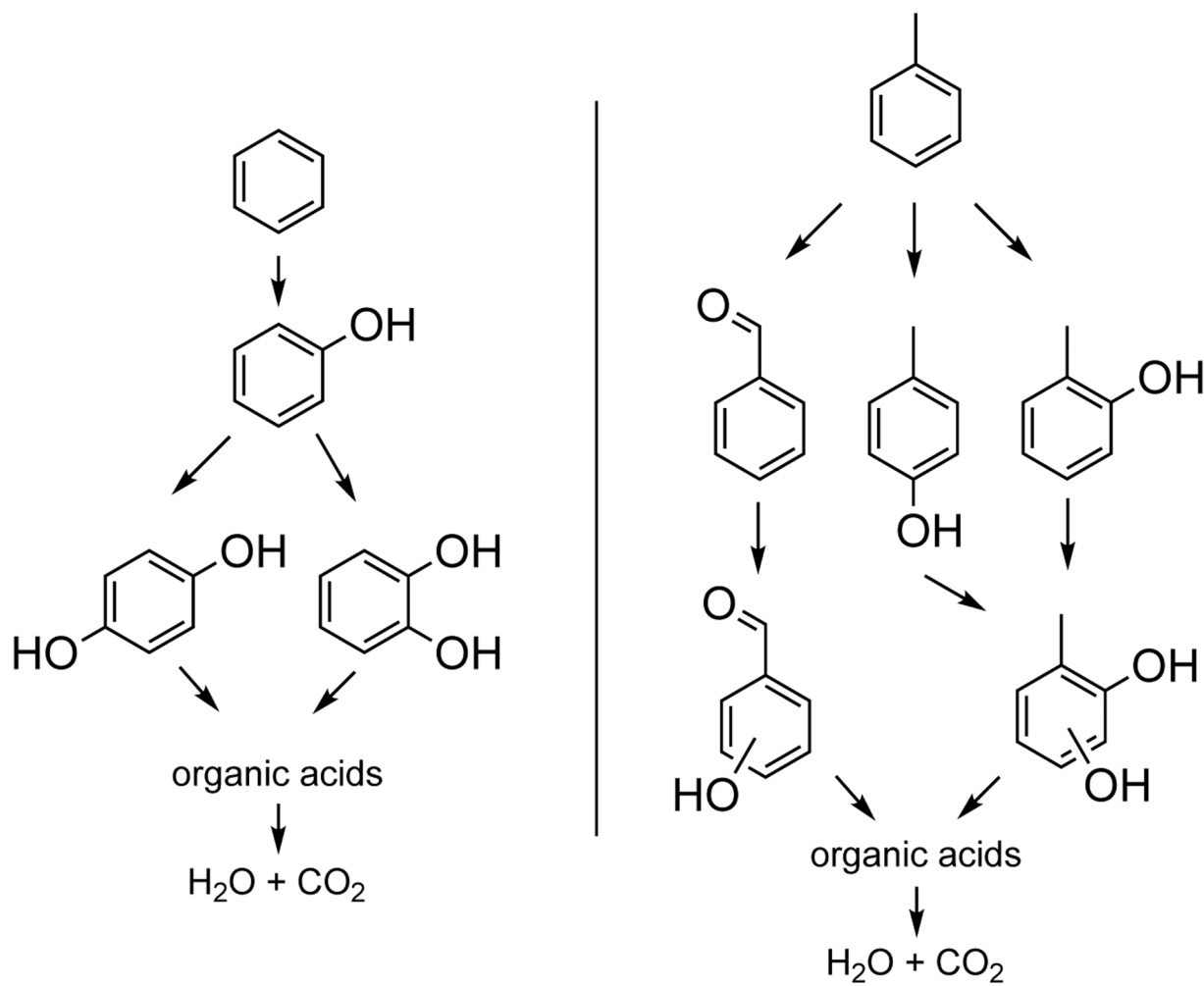


**Figure 1.** Simplified pathway based on previous studies for the transformation of benzene (left) and alkyl-substituted aromatic compounds (right) when  $\text{HO}^\bullet$  or  $\text{SO}_4^{\bullet-}$  are employed for oxidative treatment.

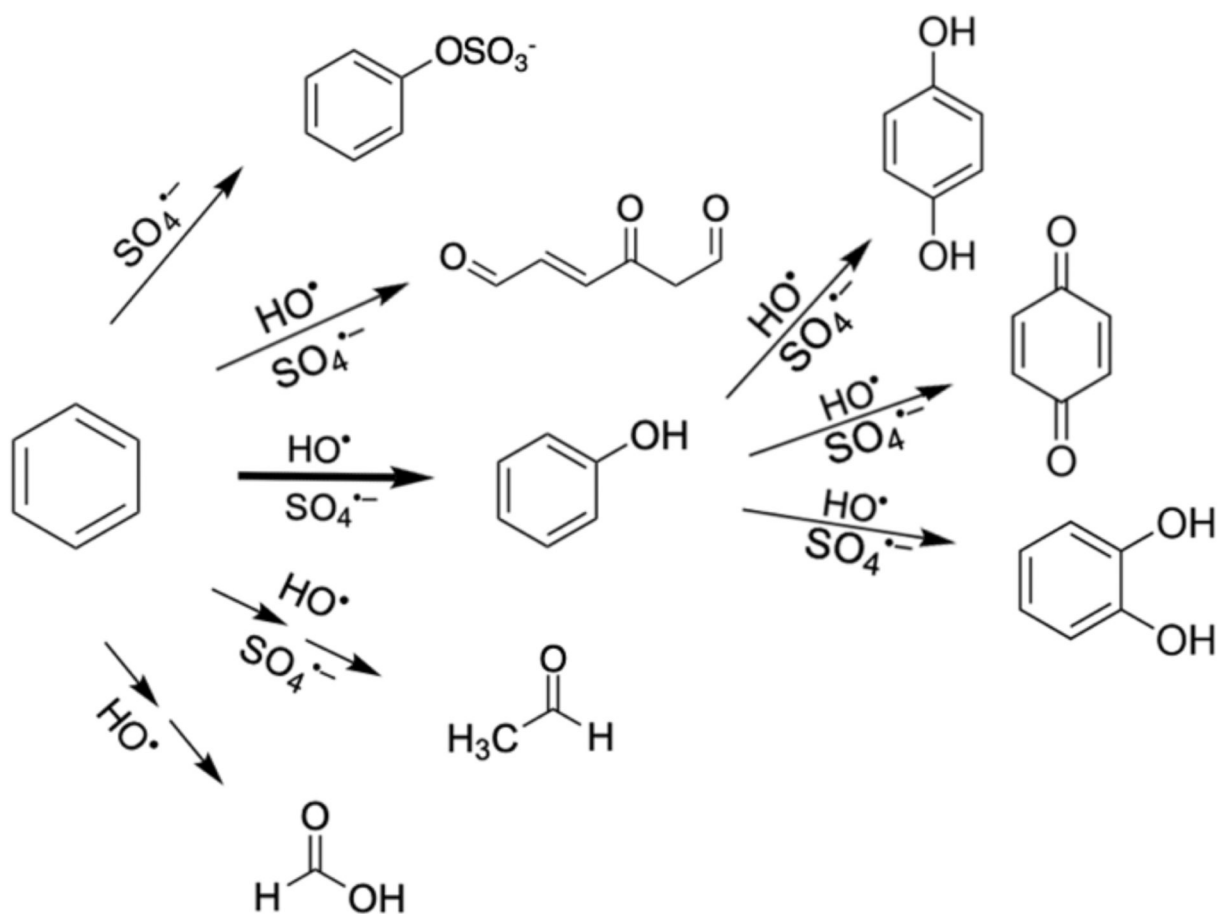


**Figure 2.** Simplified representation of the products detected from the oxidation of benzene by  $\text{HO}^\bullet$  or  $\text{SO}_4^{\bullet-}$ . Pathways indicated with two arrows indicate a more complex process that yields other products that were not quantified as part of this study.

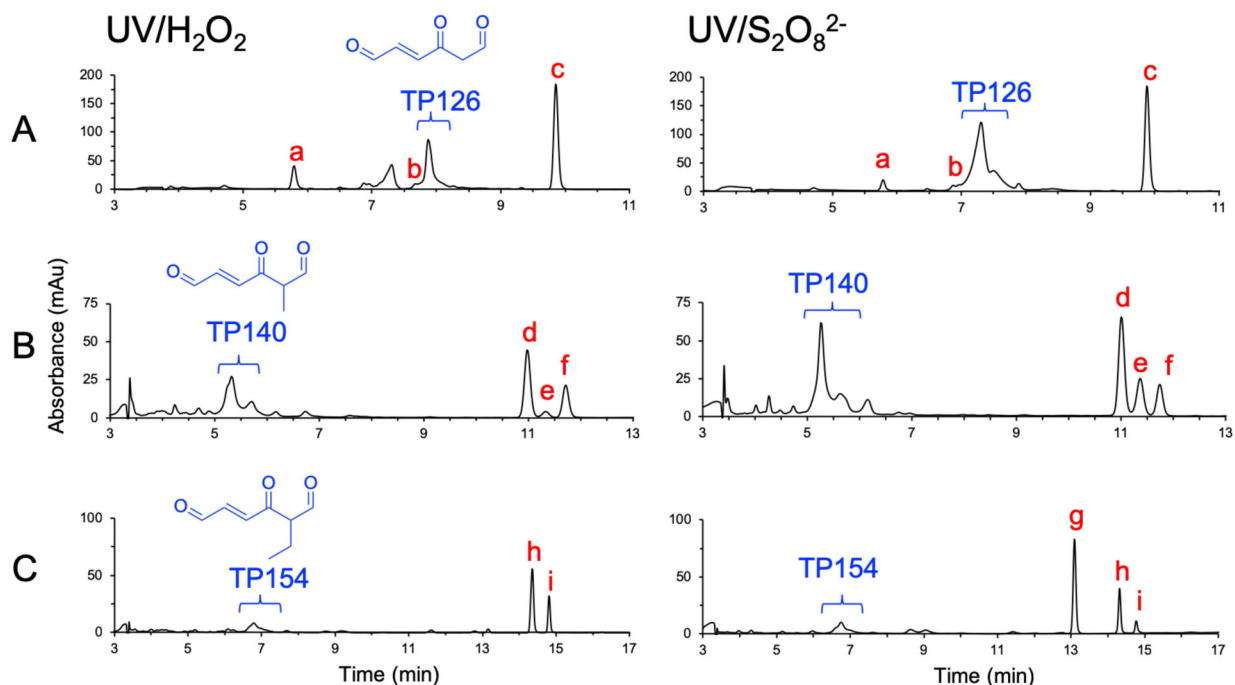


**Figure 3.**

HPLC/UV/Vis chromatograms at 280 nm of A) benzene, B) toluene, and C) ethylbenzene after 30% loss of the parent compound at pH 8 in 50 mM borate buffer by (left) HO<sup>•</sup> and (right) SO<sub>4</sub><sup>•-</sup>. Coeluting keto and enol tautomers are present in the TP126, TP140, and TP154 peaks. While only the keto-dial is pictured, the TP140 and TP154 peaks also consist of coeluting dial and enal isomers (Table S2). Quantified ring-retaining products include a) hydroquinone, b) catechol, c) phenol, d) p-cresol, e) benzaldehyde, f) o-cresol, g) acetophenone, h) p-ethylphenol, and i) o-ethylphenol.

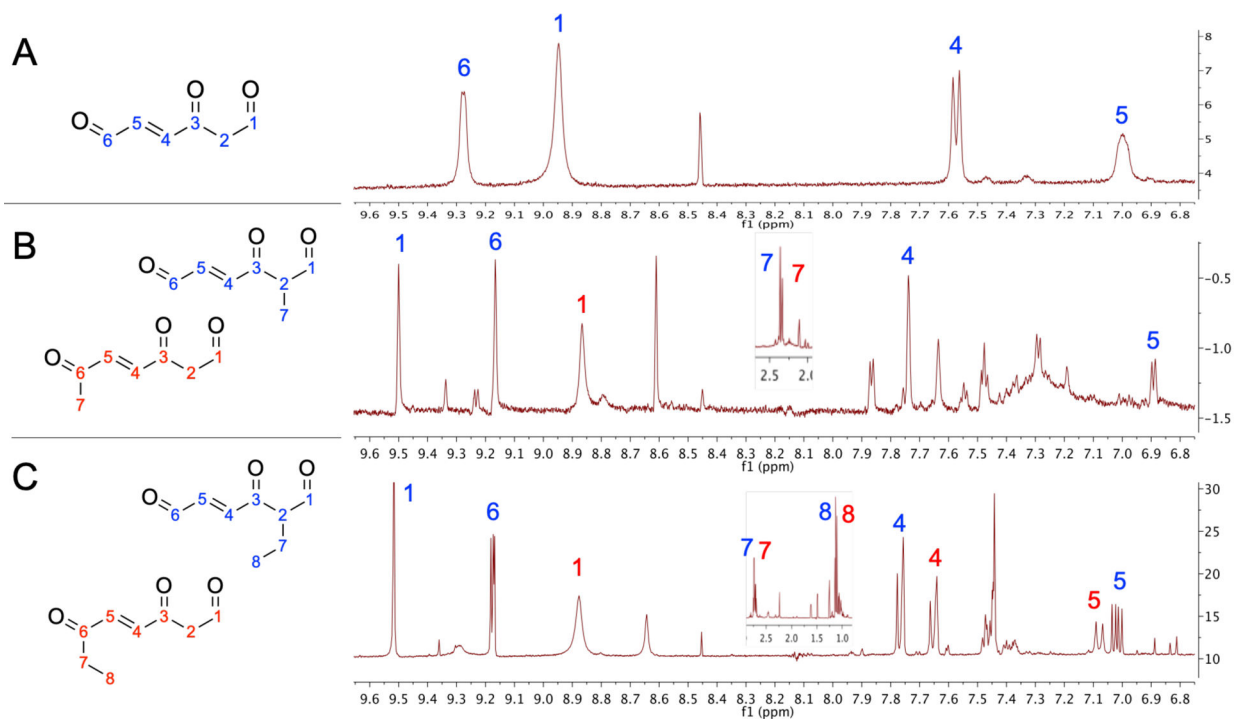


**Figure 4.**

$^1\text{H}$  NMR spectra in  $\text{D}_2\text{O}$  solvent obtained at 700 MHz with TMS as an internal reference at zero ppm for the SPE-concentrated transformation products of A) benzene, B) toluene, and C) ethylbenzene.

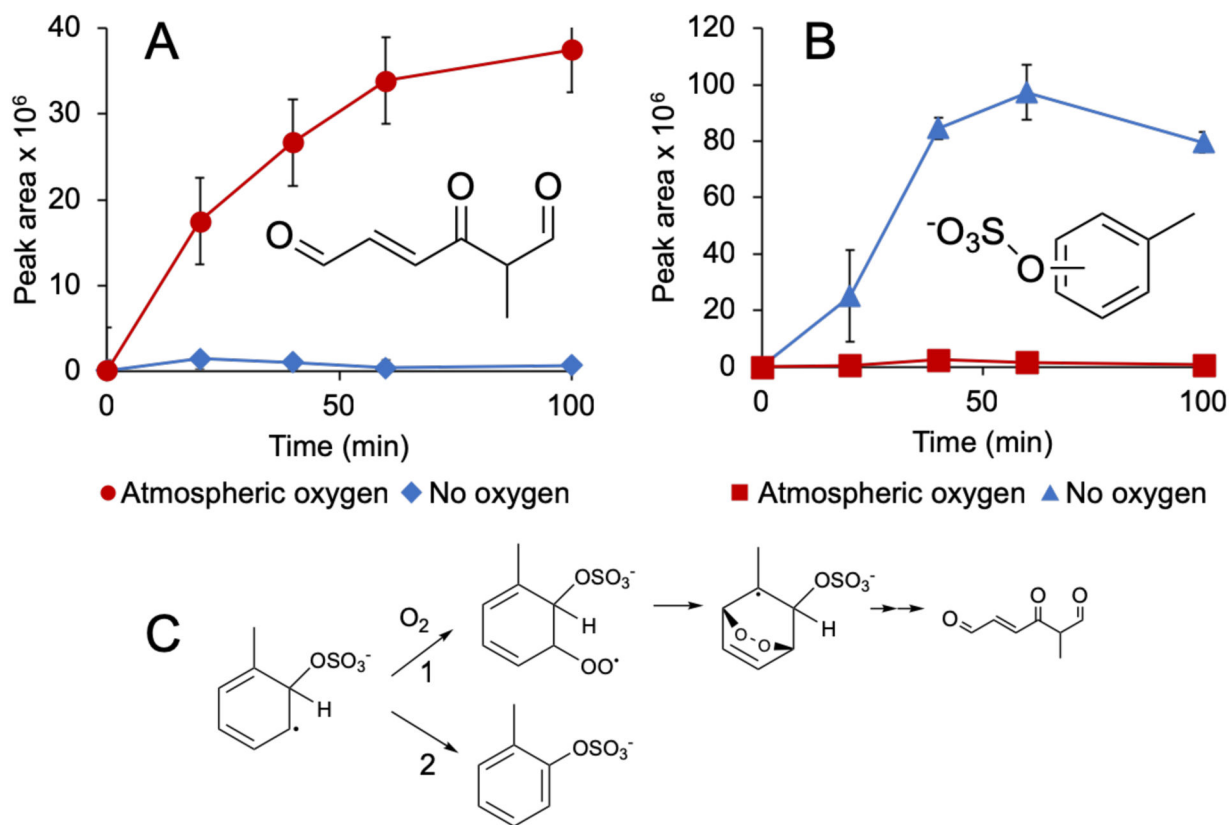


**Figure 5.**

Production of A) the ring cleavage product TP140 and B) the cresyl sulfate  $m/z$  (-) 187 from the reaction of toluene with sulfate radical in air saturated or oxygen free conditions. The reaction pathway in C proceeds through 1) the addition of oxygen to the radical intermediate, resulting in ring cleavage, or 2) in the absence of oxygen, a stable sulfate adduct.



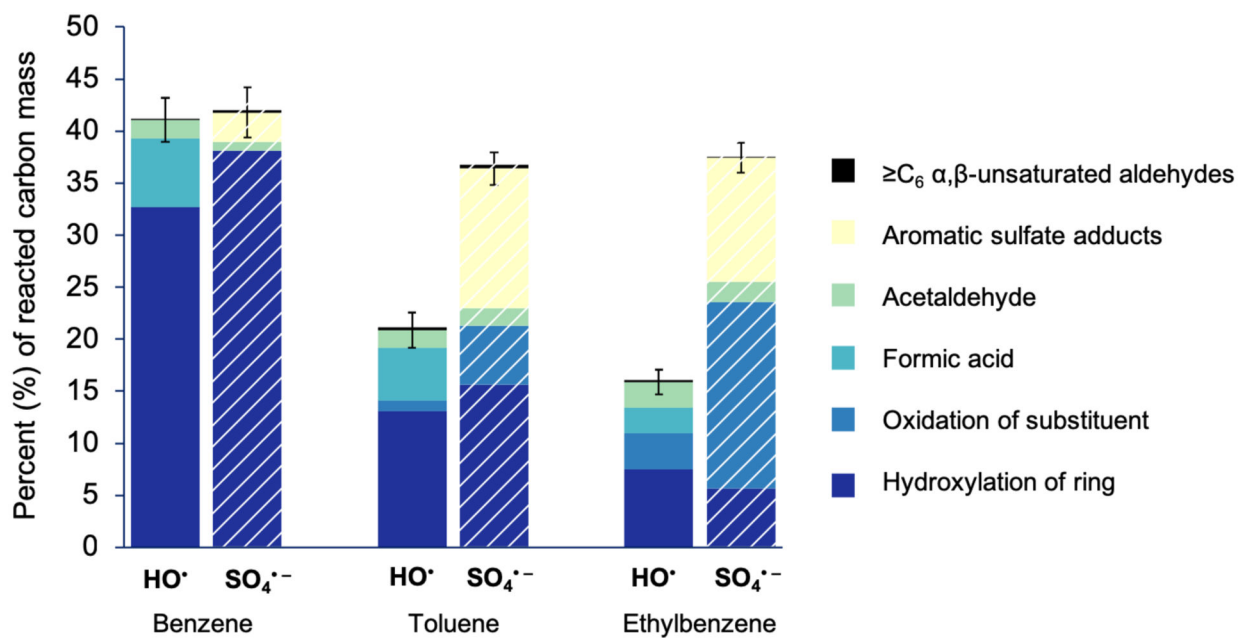


**Figure 6.** Product distribution for HO• and SO<sub>4</sub>•<sup>-</sup> oxidation of benzene, toluene, and ethylbenzene when 30% of the parent mass had been reacted. Reaction conditions: 1 mM aromatic compound, 10 mM oxidant, pH 8 with 50 mM borate.

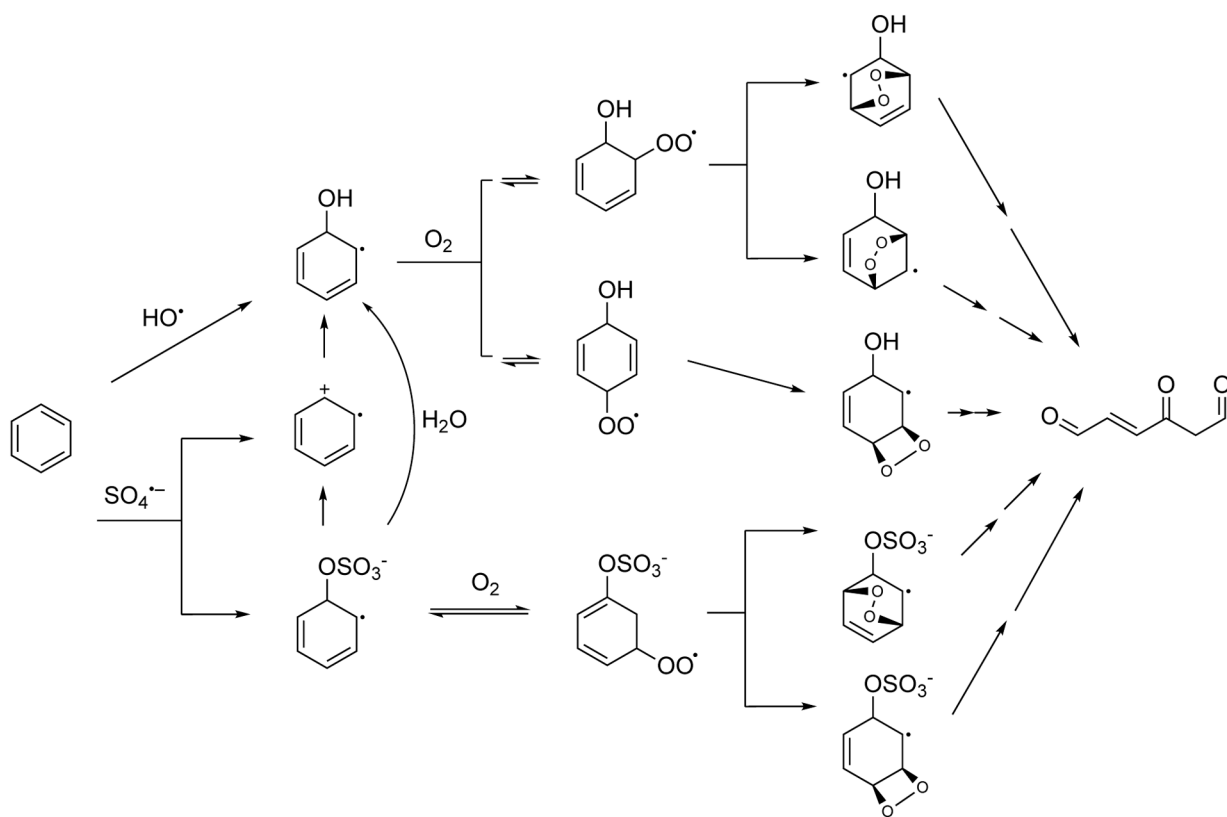


**Figure 7.** Oxidation of benzene by  $\text{HO}^\bullet$  and  $\text{SO}_4^{\bullet-}$  to form 4-oxo-2-hexenedial: pathways of ring cleavage at a single site. Final steps likely involve  $\text{O}_2$ ,  $\text{H}_2\text{O}$ , and/or an intramolecular rearrangement.